

# Computer Animation of Electron Motion in Nano-Meter Scale Devices

HANS DE RAEDT AND KRISTEL MICHIELSEN

*Institute for Theoretical Physics and Materials Science Centre  
University of Groningen, Nijenborgh 4  
NL-9747 AG Groningen, The Netherlands  
E-mail: deraedt@phys.rug.nl*

## ABSTRACT

A discussion is given of a technique to simulate the quantum mechanical motion of electrons in nano-scale devices. The results of the simulation are used to produce digital video's, facilitating the interpretation of the quantum mechanical phenomena. The power and flexibility of the simulation method is illustrated by some examples of electron emission from nano-meter scale sources.

## 1. Introduction

Experiments on atom-size field-electron-emission sources have shown that these atom-size tips act as unusual electron beam sources, emitting electrons at fairly low applied voltages (a few thousand volts or less) with a small angular spread (of a few degrees).<sup>1,2</sup> These properties make such electron sources very attractive for applications to electron microscopy, holography and interferometry.<sup>3</sup> For the materials used to fabricate the tips, e.g. tungsten, iron, gold, ..., the characteristic wavelength (i.e. the Fermi-wavelength  $\lambda_F$ )  $\lambda_F \approx 10\text{\AA}$ . A similar but otherwise unrelated development due to progress in nano-lithography is the possibility of performing "electron-optics" experiments in solid state devices.<sup>4</sup>

From physical point of view, these nano-meter scale devices share at least one important generic feature: The characteristic dimensions of these devices are comparable to the wavelength (typically the Fermi wavelength  $\lambda_F$ ) of the relevant particles (typically electrons). Under this stringent condition, a classical, "billiard-ball" description of the particle motion is no longer valid. A calculation of the device properties requires a full quantum-mechanical treatment.

## 2. Simulation method

The dynamic properties of a non-relativistic quantum system are governed by the time-dependent Schrödinger equation (TDSE)

$$i\hbar \frac{\partial}{\partial t} |\Phi(t)\rangle = \mathcal{H} |\Phi(t)\rangle \quad , \quad (1)$$

where  $|\Phi(t)\rangle$  represents the wave function of the system described by the Hamiltonian  $\mathcal{H}$ .

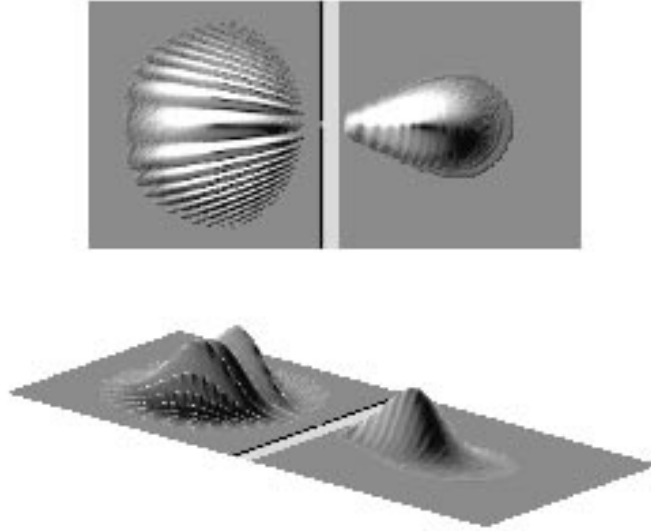


Fig.1. Intensity of the wave packet reflected and transmitted by a  $\lambda_F$ -wide aperture followed by a triangular potential barrier, a simple model for an atom-size tip. The length of the constriction is  $\lambda_F/2$ , the height and length of the potential barrier are  $1.5E_F$  and  $5\lambda_F$  respectively. The angle of incidence  $\psi = 0^\circ$ . The emitted beam is strongly focussed.

Solving the TDSE equation for even a single particle moving in a non-trivial (electromagnetic) potential is not a simple matter.<sup>5</sup> For most problems of interest, the dimension of the matrix representing  $\mathcal{H}$  is quite large (e.g.  $500000 \times 500000$  for the calculations presented in this paper) and the time-interval over which one wants to follow the motion of the particle can be large. Issues such as the stability, accuracy, and conservation of probability impose the use of algorithms tuned to the TDSE.<sup>5</sup>

We have developed an algorithm<sup>6</sup> to solve the TDSE based on the so-called fractal decomposition formula proposed by Suzuki.<sup>7</sup> The algorithm that we use is accurate to fourth-order in both the spatial and temporal mesh size and unconditionally stable.<sup>6</sup> Additional technical details can be found elsewhere.<sup>6</sup> In practice we solve the TDSE subject to the boundary condition that the wave function is zero outside the simulation box, i.e. we assume perfectly reflecting boundaries. Special attention has been given to techniques to present the results of these massive computations in a comprehensible manner. Visualization and animation techniques are used to generate digital video's, thereby greatly facilitating the interpretation of the simulation results.

TDSE solvers have been employed to study a variety of problems including electron emission from nanotips,<sup>8,9,10</sup> Andreev reflection in mesoscopic systems,<sup>11,12</sup> the Aharonov-Bohm effect,<sup>13,14</sup> quantum interference of charged identical particles,<sup>15,14</sup> etc.. Appealing features of the TDSE approach are that it is extremely flexible in that it can handle arbitrary geometries and (vector) potentials and that its numerical stability and accuracy are such that for all practical purposes the solution is exact. It provides a unified framework to investigate various quantum phenomena in which diffraction, interference and/or tunneling is important.

### 3. Applications<sup>16</sup>

As already mentioned above, experiments on atom-size tips<sup>1,2</sup> have demonstrated that they act as unusual electron beam sources, emitting electrons at fairly low applied voltages with a small angular spread. The simplest model of a single-atom tip consists of a constriction (the atom) followed by a triangular barrier (the metal-vacuum potential). The triangular barrier is higher than the energy of the waves inside the source. To leave the source the electron has to tunnel through the barrier. The solution of a (much simplified) model that captures the basic physics is highly non-trivial. The simulation approach discussed above has been instrumental to unravel the mechanism that leads to the experimentally observed behavior.

A two-dimensional model is sufficient to investigate the various possible mechanisms. We have solved the corresponding TDSE on a grid of  $1024 \times 513$  points with mesh size  $\delta = \lambda_F/10$ , using a time step  $\tau = 0.03125\hbar/E_F$  where  $E_F$  is the Fermi energy, and 4096 time steps. Incident waves were chosen to be Gaussians of width  $6\lambda_F \times 6\lambda_F$ , sufficiently large to mimic a plane wave front impinging on the emission area. Simulations (not shown) demonstrate that the observed behavior does not change if the width of the Gaussian is increased further.

Fig.1 demonstrates that tunneling is a very effective focussing mechanism. Although it reduces the intensity of the emitted beam significantly, the diffraction generated at the exit plane of the small aperture is considerably suppressed by the tunneling mechanism. Extensive theoretical work<sup>8,17</sup> revealed that tunneling through the metal-vacuum potential is the main physical mechanism determining the unusual properties of the emitted electron beams.

Another remarkable feature of the iron atom-size tips is that at temperatures above the Curie-temperature they emit a single beam whereas below the Curie-temperature two well-separated electron beams emerge.<sup>18</sup> Tungsten or gold tips do not exhibit this behavior. This suggests that at temperatures below the Curie-temperature the electron beams may be spin-polarized.

Simulations (not shown) rule out a Stern-Gerlach type of mechanism: The magnetic field at the apex, required to split the electron beam, has to be unrealistically large. Some simulation results for an alternative mechanism are shown in Figs.2,3. Here we have assumed that the tip is magnetized in a certain (arbitrary) direction. Experimentally the strength of the field is unknown so we have taken (several) values that seem “reasonable”. In Fig.2 we show the initial state of the spin-up (light) and spin-down (dark) part of the wave function. Both parts have been superimposed by means of image processing techniques. In this case the initial direction is set from left to right. The tip is modelled by a small aperture, followed by a triangular barrier. The magnetic field (dark grey) is present in the tip and extends a little outside. The light grey area represents the vacuum region.

In the region where the field is non-zero the electron (for both spin-up and spin-down) will experience the Lorentz force. Consequently it will make a bend. From the computer animation (see talk) it is obvious that the tunnel barrier does NOT affect the direction of the electron as it leaves the region where the magnetic field is non-zero. As shown in Fig.3 there is NO splitting of the beam due to the spin of the electron, although due to

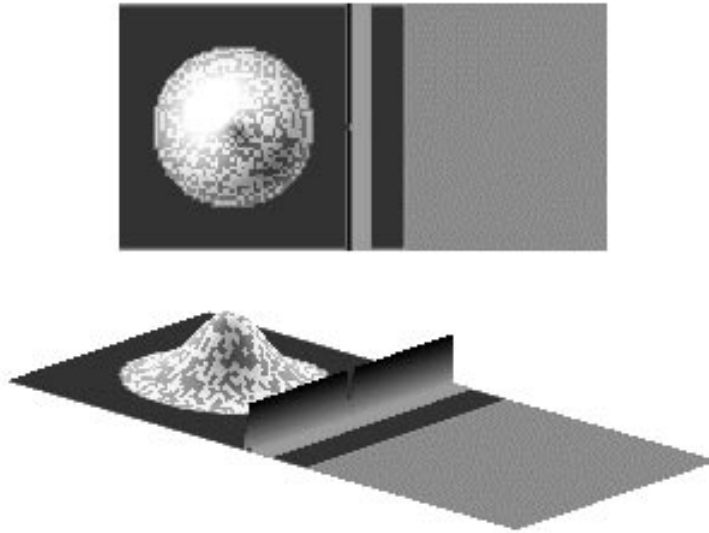


Fig.2. Initial state of the spin-up (light) and spin-down (dark) electron in a model for a magnetized atom-size tip. The small aperture and the triangular barrier represent the atom-size emission source. The magnetic field is present in the dark grey area only. Initially the waves move from left to right.

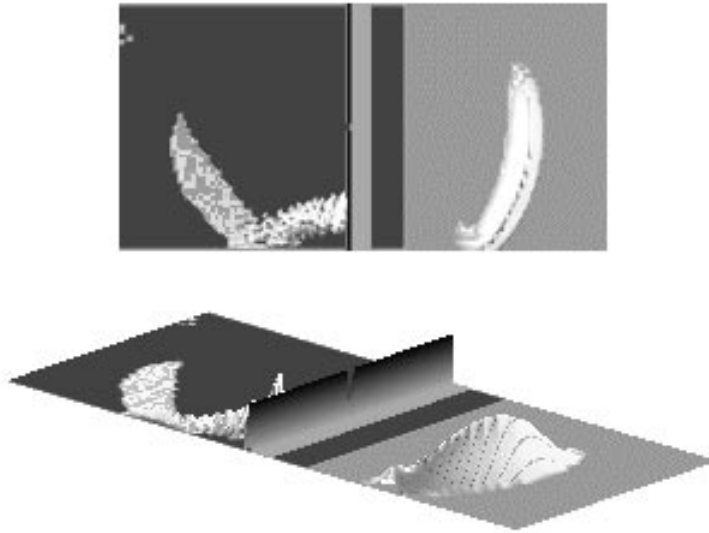


Fig.3. Initial state of the spin-up (light) and spin-down (dark) electron in a model for a magnetized atom-size tip. The small aperture and the triangular barrier represent the atom-size emission source. The magnetic field is present in the dark grey area only. The initial waves move from left to right. The deviation of the electron trajectory from a straight left-to-right line is due to the Lorentz force inside the tip. There is no directional splitting of the waves due to the electron spin.

the Zeeman interaction, the energy of the emitted spin-up and spin-down wave differ. For this mechanism to explain the experimentally observed features it is necessary that the direction of magnetic field at the apex oscillates with time. Whether this happens or not is an open question.

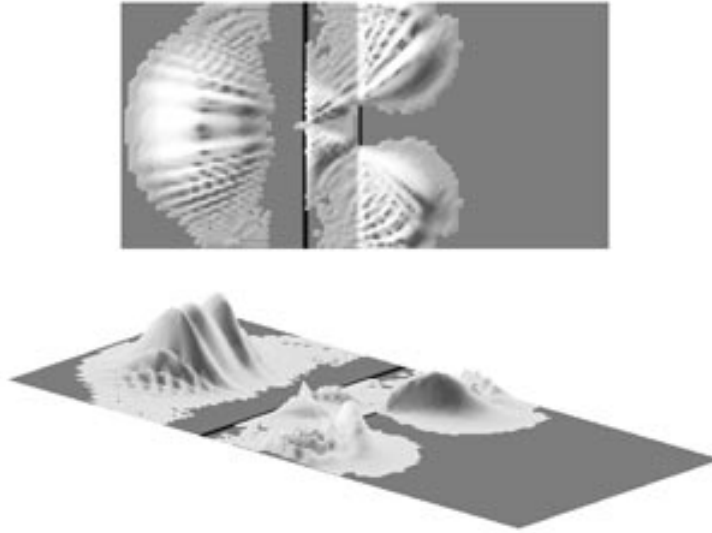


Fig.4. Scattering of a Gaussian wave packet by an object of size  $\lambda \times 8\lambda$ , under conditions appropriate for Fresnel diffraction. The image (not shown) on a screen placed far to the right, produced by the scattered wave does not show the features characteristic for Fresnel diffraction.

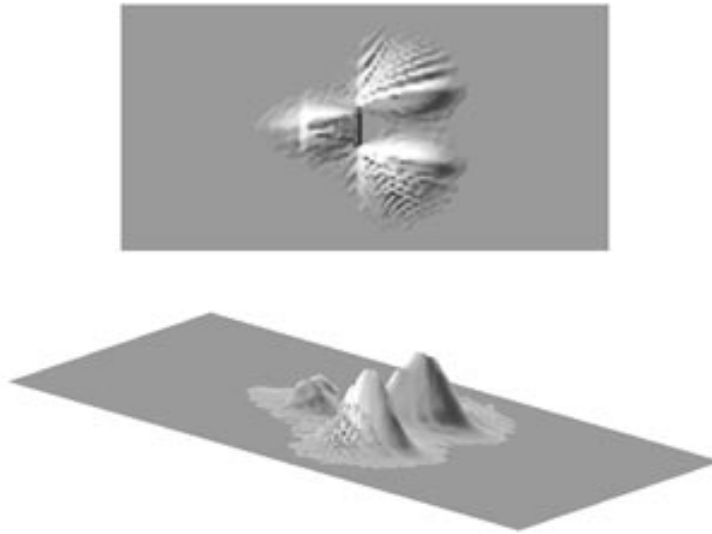


Fig.5. Scattering of wave packet, emitted by a small aperture, by an object of size  $\lambda \times 8\lambda$ , under conditions appropriate for Fresnel diffraction. The image (not shown) on a screen placed far to the right, produced by the scattered wave shows all the features characteristic for Fresnel diffraction.

Finally we illustrate the use of the simulation technique to study the process of image formation in the Fresnel Projection Microscope<sup>19</sup> In the experiment the source-sample distance is small ( $\approx 10\text{nm}$ ) and a theoretical description requires at least a calculation of the Fresnel-Kirchoff integral. The latter requires as input, a guess for the profile of the incident beam. In Figs.4,5 we show the results of TDSE simulations for the case of a Gaussian wave packet (Fig.4) and an wave emerging from a tip (Fig.5) impinging on a object of size  $\lambda_F \times 8\lambda_F$ . The image produced on a screen placed far ( $\approx 10\text{cm}$ ) at the right

is computed from the TDSE solution by a technique described in ref.<sup>20</sup>. Our results show that in order to observe the Fresnel-like behavior it is necessary to use a profile for the beam, different from a Gaussian: The spreading of the minimum-uncertainty wave packet apparently is not strong enough to produce the fringes typical for Fresnel diffraction.

## 4. Conclusions

The simulation software described in this paper is a powerful tool to investigate various aspects of wave mechanical phenomena in nano-meter scale devices. Supplemented by computer animation techniques the simulation provide direct and intuitively clear insight into the physical behavior of these systems.

## 5. Acknowledgements

This work is supported by Dutch and EEC funding agencies.

## 6. References

1. Vu Thien Binh and J. Marien, *Surface Science* **102** (1988) L539.
2. Vu Thien Binh, *J. Microscopy* **152** (1988) 355.
3. M.P. Silverman, W. Strange, and J.C.M. Spence, *Am. J. Phys.* **63** (1995) 800.
4. S. Washburn, *Nature* **343** (1990) 415.
5. H. De Raedt, *Comp. Phys. Rep.* **7** (1987) 1.
6. H. De Raedt, and K. Michielsen, *Computers in Physics* **8** (1994) 600.
7. M. Suzuki, *J. Math. Phys.* **32** (1991) 400.
8. N. García, J.J. Sáenz, and H. De Raedt, *J. Phys.: Condens. Matter* **1** (1989) 9931.
9. H. De Raedt, and K. Michielsen, *Nanosources and Manipulation of Atoms Under High Fields and Temperatures: Applications*, edited by Vu Thien Binh, N. García and K. Dransfeld, (NATO-ASI Series, Kluwer, 1993).
10. K. Michielsen and H. De Raedt, “Electron Focussing”, Multimedia Presentation. For more information send e-mail to the first author.
11. H. De Raedt, K. Michielsen, and T.M. Klapwijk, *Phys. Rev.* **B50** (1994) 631.
12. H. De Raedt and K. Michielsen, “Andreev Reflection”, Multimedia Presentation. For more information send e-mail to the first author.
13. H. De Raedt and K. Michielsen, *Comp. in Phys.* **8** (1994) 600.
14. K. Michielsen and H. De Raedt, “Quantum Mechanics”, Multimedia Presentation. For more information send e-mail to the first author.
15. H. De Raedt and K. Michielsen, *Ann. Physik* **4** (1995) 697.
16. Based on work carried out in collaboration with N. Garcia, J.J. Saenz, and Vu Thien Binh.
17. J.J. Sáenz, N. García, Vu Thien Binh, and H. De Raedt, *Scanning Tunneling Microscopy and Related Methods*, edited by R.J. Behm et al, (Kluwer Academic, Dordrecht, 1990).
18. Vu Thien Binh *et al.* (unpublished).
19. Vu Thien Binh, V. Semet, and N. García, *Appl. Phys. Lett.* **65** (1994) 2493.

20. K. Michielsen, and H. De Raedt, *J. Phys.: Condens. Matter* **3** (1991) 8247.